AAEC/E236

AUSTRALIAN ATOMIC ENERGY COMMISSION

RESEARCH ESTABLISHMENT
LUCAS HEIGHTS

A COMPARISON OF MEASURED AND CALCULATED $^{238}U/^{235}U$ FISSION RATE RATIOS FOR NATURAL UO_2 ROD-CLUSTER FUEL ELEMENTS IN THE ZERLINA REACTOR

by

G. DURANCE
D.B. McCULLOCH

August 1972

ISBN 0 642 99477 3

AUSTRALIAN ATOMIC ENERGY COMMISSION

RESEARCH ESTABLISHMENT

LUCAS HEIGHTS

A COMPARISON OF MEASURED AND CALCULATED $^{238}U/^{235}U$ FISSION RATE RATIOS FOR NATURAL UO_2 ROD-CLUSTER FUEL ELEMENTS IN THE ZERLINA REACTOR

by

G. Durance

D. B. McCulloch

ABSTRACT

Experimentally measured values of the $^{238}U/^{235}U$ fission rate ratio δ_{28} in uranium dioxide cluster fuel elements in a heavy water moderated, light water cooled reactor lattice configuration are compared with the predictions of one-group Monte Carlo cell calculations (MONTE), corrected for the actual experimental environment. A comparison between MONTE and WIMS calculations for the experiments is also given.

National Library of Australia card number and ISBN 0 642 99477 3

The following descriptors have been selected from the INIS Thesaurus to describe the subject content of this report for information retrieval purposes. For further details please refer to IAEA–INIS–12 (INIS: Manual for Indexing) and IAEA–INIS–13 (INIS: Thesaurus) published in Vienna by the International Atomic Energy Agency.

CYLINDRICAL CONFIGURATION; DATA; FISSION RATIO; FUEL ELEMENT CLUSTERS; FUEL RODS; LEAST SQUARE FIT; M CODES; MONTE CARLO METHOD; ONE–GROUP THEORY; POWER DENSITY; REACTOR LATTICES; URANIUM DIOXIDE; URANIUM 235; URANIUM 238; W CODES; ZERLINA REACTOR

CONTENTS

1. INTRODUCTION

As part of an investigation of the adequacy of the METHUSELAH method (Alpiar 1964, Brinkworth and Griffiths 1966) of lattice calculation for boiling light water cooled heavy water moderated reactors, a one-group Monte Carlo code, MONTE, was written and used by McCulloch, Doherty and Hesse (1968) to calculate values of the $^{238}U/^{235}U$ fission rate ratio, δ_{28}, for comparison with the then existing published data for UO_2 rod cluster fuelled heavy water lattices.

As a result of that investigation, it was considered desirable to conduct a series of experiments in which δ_{28} would be measured for a range of cluster geometries and light water coolant densities using a common technique. Such a programme has since been carried out (Rose, Jain and Menezes 1972) on a collaborative basis between AAEC and IAEC, using the latter's zero energy heavy water moderated reactor ZERLINA at the Bhabha Atomic Research Centre, Trombay, India.

This report compares the results of Rose et al. with predictions of the MONTE code, and also with those of a version of the UKAEA reactor analysis code WIMS (Askew, Fayers and Kemshell 1966). The direct results of both MONTE and WIMS codes are adjusted before the comparison via METHUSELAH/CRAM (Hassitt, 1962) calculations to take account of the actual experimental environment provided by the ZERLINA reactor.

2. EXPERIMENTAL DATA

The core configuration of ZERLINA used for the δ_{28} measurements has been described by Rose et al. The important feature for the present work, is that each experimental cluster was located on the axis of the reactor in a D_2O region 57 cm square, bounded in turn by the normal ZERLINA single metal-rod fuelled lattice of 19 cm square pitch.

Details of each experimental cluster/coolant combination are given by Rose et al. whose cluster nomenclature is retained in this report. Their results for cluster average and individual rod δ_{28} values are summarised in Tables 1 and 2.

3. CALCULATIONS

The object of the present theoretical study was to compare Rose et al.'s experimentally measured values of δ_{28} with those calculated by the MONTE code. This necessitated a correction to the MONTE calculated values to allow for the effects of the non-similar lattice cells surrounding the experimental cluster in the ZERLINA reactor.

It was anticipated that this could be done using METHUSELAH cell calculations to provide averaged cross sections for use in the CRAM diffusion code.

However, MONTE assumes an infinite lattice of identical cells and calculates directly the number of fissions in ^{238}U arising from one ^{235}U fission distributed within the cluster in accordance with the relative rod power distribution as given by METHUSELAH. It is therefore not directly comparable with a normal 'k_∞' calculation in which the eigenvalue is obtained by adjustment of the fission source. Since the correction factor to be applied to MONTE is derived by comparison of infinite lattice and ZERLINA calculations, considerable care is therefore required in choice of the infinite lattice model.

In practice, the infinite lattice was represented in CRAM in cylindrical geometry as a central cell with separate fuel and moderator regions, surrounded by a sufficiently large array of 'smeared' similar cells, the whole being made critical by a further surrounding driver or absorber region. Extensive investigations were made of this type of representation to ensure that the methods adopted to achieve criticality were not significantly affecting the value of δ_{28} calculated in the central cell.

3.1 Experimental Cluster Lattice Cell Calculations

For each experimental cluster a five-group METHUSELAH II (Brinkworth and Griffiths, 1966) calculation was done for a 57 cm square pitch infinite lattice. This gave cell averaged cross sections for use in subsequent CRAM calculations, and normalised rod fission source distributions for use in MONTE.

In addition, the cell averaged cross section data were condensed to four groups and separated by appropriate flux and volume weighting into a cross section set appropriate to the fuelled region within the pressure tube, and a set for the remainder of the cell. These separated data were used for the central cell representation in CRAM for both the ZERLINA reactor and the pseudo infinite lattice models.

3.2 Psuedo Infinite Lattice Calculations

In order to derive correction factors to be applied to MONTE values of δ_{28}, it is necessary to compare the δ_{28} value calculated for the central lattice cell of ZERLINA, with that for the same cell at the centre of a pseudo-infinite critical array of similar cells.

It is to be expected that the value of δ_{28} derived for the central cell may depend on the representation of the surrounding cells, and the method by which the system is made critical. Accordingly, an extensive investigation was made to arrive at a satisfactory model to represent the situation. Figure 1a augments the descriptions of the infinite lattice models which follow in this section.

In all cases, the central experimental cell was represented in a one-

dimensional cylindrical CRAM model using the separated fuel and moderator cross section data as described in section 3.1. The surrounding similar cells were represented by the cell-averaged METHUSELAH II cross section data, condensed again to four energy groups. The thickness of this surrounding region was initially set at five migration lengths, which it was believed would be adequate to ensure that spectral transients from the outer edge, or from any outer driver region, would be removed before the boundary of the central cell was reached.

Initially, the model as described was given a reflective boundary condition, and a 'k_∞' calculation made for each test cluster. A mesh size investigation was then made, and it was established that the central cluster neutron energy spectrum and δ_{28} were quite sensitive to the spacing of mesh points in the immediate surrounding D_2O region. As a result, 40 mesh intervals were allotted to this region, being a number more than adequate to ensure that the results were converged with respect to mesh interval.

The thickness of the smeared cell region was then varied from its starting value of five migration lengths down to three migration lengths. The mesh size in this region was also changed from 5 to 10 cm, and in no case were δ_{28} changes greater than 1 part in 10,000 observed. These results confirmed that the region size and mesh interval chosen were adequate to ensure convergence of the central cluster δ_{28} values.

It was now necessary to investigate methods of making this infinite lattice model just critical. For those cases where $k_\infty > 1$, three methods of achieving criticality were investigated:

(a) The reflected outer boundary condition was maintained, and an axial buckling superimposed to give $k_{eff} = 1$.

(b) The outer radial boundary was freed, and a radial mesh size search made in the smeared region to give $k_{eff} = 1$.

(c) An additional 10 cm annulus of the smeared cell data was added at the existing outer boundary, and this new region was poisoned with cadmium, until k_{eff} for the system reached unity while retaining a reflected condition at the new outer boundary.

δ_{28} values for the central cluster by methods (b) and (c) were essentially identical, whilst those by method (a) were lower by up to one half per cent. Since some of the axial bucklings for criticality were rather unrealistic, and models (b) and (c) were closer in concept to the ZERLINA reactor model and also to the $k_\infty < 1$ infinite lattice model, model (c) was adopted.

For the $k_\infty < 1$ cases, a driver region containing ^{235}U and D_2O plus an 80 cm thick D_2O reflector region with a free boundary were added outside the five migration length thick smeared METHUSELAH II data region. The driver region cross sections were obtained from GYMEA (Pollard and Robinson, 1966) for a $^{235}U/D_2O$ volume fraction of 10^{-4}, and the radial mesh vector in the driver region of the CRAM model adjusted to achieve criticality.

For both $k_\infty > 1$ and $k_\infty < 1$ cases, 'critical infinite lattice' models had now been established for which δ_{28} in the experimental cluster was converged with respect to (i) method of achieving criticality, (ii) mesh representation, and (iii) smeared region thickness. Furthermore, the adopted models conformed sufficiently closely to appropriate models for ZERLINA, that any residual small errors in representation would be likely largely to cancel when the ZERLINA and pseudo infinite lattice values of δ_{28} were compared to give correction factors for MONTE.

One further feature remained to be checked. The use of smeared cell data in the region immediately surrounding the central cell meant that fuel was closer to the experimental cluster in the model than would be the case in an infinite lattice. Accordingly, the ring of cells immediately surrounding the experimental cell was represented by a ring of D_2O, a ring of fuel/D_2O mixture, and another ring of D_2O before passing into the smeared cell representation. The central cluster values of δ_{28} were not significantly affected by this change, confirming that the smeared cell model directly surrounding the central cell is adequate.

The final values of δ_{28} derived for the infinite lattice with the METHUSELAH/CRAM models described are given in Table 1.

3.3 ZERLINA Calculations

The central experimental cell was represented exactly (including number of mesh points) as described above for the pseudo infinite lattice calculations. Both one-dimensional and two-dimensional CRAM models were then used to represent the reactor. The regions used in the one-dimensional model are illustrated in Figure 1b.

In the one-dimensional calculations, cell-average four group cross sections for the metal rod fuelled ZERLINA lattice cell, the D_2O reflector, aluminium tank and graphite reflector, were available (Manning, unpublished) and were used in a CRAM calculation with a typical experimental cluster represented in the reactor central cell. An axial buckling search was made for criticality, giving group dependent bucklings which were used in the GYMEA-WDSN-GYMEA sequence to yield new cell-average cross section data for the

ZERLINA metal rod lattice. These new cross sections were then used to represent the reactor with each experimental cluster in turn at the centre, giving the METHUSELAH/CRAM 'ZERLINA δ_{28}' values of Table 1.

The validity of these one-dimensional ZERLINA calculations was checked using a two-dimensional R,Z CRAM model due to Manning (unpublished). First, the reactor with a (cylindricised) 57 cm square D_2O region at its centre was represented using its actual measured critical height, and criticality achieved by slight 1/v poisoning of the bottom graphite reflector. This configuration was then truncated at the outer boundary of the metal-fuelled region using appropriate boundary conditions derived from the CHOPOFF (Manning, unpublished) and DIFF (Spinks and Manning 1967) codes to represent the regions so removed. The resulting model enabled a large number of mesh-points to be used in the central (experimental) region for subsequent calculations without making the computing time excessively long.

For a representative range of experimental clusters, the appropriate cluster data and measured critical heights were inserted in the above R,Z model, and k_{eff} calculations made. After correction for slight departures from $k_{eff} = 1$, the δ_{28} values derived were in excellent agreement with those from the one dimensional calculations.

3.4 MONTE Calculations

The METHUSELAH cell calculations referred to in section 3.1 provided fast group (> 0.821 MeV) cross section data and rod power peaking factors for each rod cluster. These were used in the MONTE code with reflected 57 cm square pitch boundary conditions to give the MONTE infinite lattice δ_{28} value for each cluster.

The latter values, $(\delta_{28})_\infty$, were multiplied by the corresponding $\frac{(\delta_{28})\ \text{CRAM-ZERLINA}}{(\delta_{28})\ \text{CRAM}_\infty}$ ratio to give the values of δ_{28} appropriate for MONTE/experiment comparison. The maximum correction was less than 0.6 per cent.

3.5 WIMS Calculations

WIMS (Askew et al., 1966) cell calculations were carried out for each experimental cluster using the DSN transport option with a radial buckling search to give $k_{eff} = 1$ for the cell. The WIMS 69-group data library was condensed to 18 groups for the DSN transport calculation, with group boundaries as given in Table 3. The effective width model (WIMS option 8002) for deuterium, the Nelkin model (WIMS option 2001) for hydrogen and the Yiftah, Okrent and Moldauer (1960) based ^{238}U data (WIMS option 2238) were the cross section options selected for the calculations.

The cluster-average δ_{28} values so obtained were corrected for the ZERLINA environment in the same way as the MONTE calculations, by use of the CRAM ZERLINA/CRAM$_\infty$ δ_{28} ratio.

4. RESULTS

Cluster-average δ_{28} values for each fuel element studied as calculated for

(a) the pseudo infinite lattice (CRAM)

(b) the ZERLINA reactor (CRAM)

(c) reflected cell (MONTE)

(d) environment corrected MONTE, and

(e) environment corrected WIMS

are given with the corresponding experimental δ_{28} values in Table 1. Since only the ratio of (a) and (b) values is of interest, the ^{238}U fast cross section data used in the METHUSELAH calculations were not adjusted from the basic library values. This is the reason for the large difference between (c) and (a) or (b) values of δ_{28}.

Experimental and MONTE δ_{28} values for individual rings of rods are given in Table 2.

5. COMPARISON OF EXPERIMENTS AND MONTE CALCULATIONS

A comparison of the cluster-average δ_{28} values obtained by Rose et al. with the corresponding MONTE δ_{28} values was made by a least-squares fitted regression line constrained to pass through the origin so that

$$\delta_{28}(\text{expt}) = A\ \delta_{28}(\text{MONTE})$$

where the slope 'A' is essentially the factor by which the ^{238}U fission cross-section used in the MONTE calculations should be scaled to give best agreement with the experimental data.

The result of this process is shown by the data of Table 4, and by Figure 2. An approximate allowance has been made in the fit for the uncertainty in the MONTE δ_{28} values (X) by combining their standard deviations in quadrature with the corresponding experimental uncertainties quoted by Rose et al., to give the DY of the table. The DY differ only slightly from the Rose et al. values since the experimental errors are generally much larger than the standard deviations of the MONTE calculations. An excellent fit is obtained with A = 1.050 $\pm$ 0.010, and a χ^2 of 8.5 for 19 degrees of freedom. It is thought that the high probability of the fit ($P(\chi^2) \simeq 0.98$) reflects the inclusion of the common calibration factor systematic error allowance in each of the results.

Since a prime objective of Rose et al.'s experiments was to provide δ_{28}

values for a wide range of clusters using a common technique so that all would be subject to the same systematic errors (as for example in P(t)), the way in which the experimental results are presented by Rose et al. and used in the above fitting process does not form the most stringent possible test of the ability of MONTE to predict trends in δ_{28} with changing geometry, coolant, etc.

We have therefore re-analysed the data of Rose et al. to extract the most precise indication of trends in δ_{28}, untramelled by systematic errors which affect only the absolute values and uncertainty thereon. We have accepted Rose et al.'s conclusion from intercomparison of results from similarly located rods within the clusters, that the uncertainty on an individual rod δ_{28} for either the Ge(Li) or NaI detector data is approximately $\pm$ 4 per cent, and that this is attributable to some unassigned source of random error. The ratio $F = \delta_{28}(\text{Ge(Li)})/\delta_{28}(\text{NaI})$ was then formed for each measured rod position and its mean value, $\overline{F} = 0.999$ found. Since the calibrating factor (P(t)) is most accurately known for the Ge(Li) data set, it is convenient to regard that set as providing the best basis for eventual absolute values. The NaI set of individual rod values was therefore scaled by the factor $\overline{F}$ to bring them to an absolute level directly comparable with the Ge(Li) data, and the mean of the two sets was obtained. Since Rose et al.'s analysis showed the unassigned random error component in each set of data to be so much larger than the accountable components, it is considered that there is a high likelihood that it was due to some in-reactor effect on the foils themselves, and therefore probably systematic to both sets of data. The errors of the individual rod δ_{28} values were therefore not reduced when the mean of the two data sets was found, but were left at $\pm$ 4 per cent.

The resulting individual rod mean δ_{28} values were then combined in the standard way following Rose et al. to give cluster average δ_{28} values and associated standard deviations. As expected, the δ_{28} values differ only marginally from those quoted by Rose et al., but the standard deviations are much smaller, reflecting the elimination of the common calibration factor systematic component. They now represent the precision with which the experimental data can indicate trends of δ_{28} with changes of cluster geometry, etc., disregarding uncertainties in the absolute values of δ_{28} attributable to uncertainties in calibration factors, foil enrichment, etc.

The revised δ_{28} values and standard deviations after combination in quadrature with the corresponding MONTE calculation standard deviations are given by the Y1 and DY1 columns respectively of Table 5, which also gives the

details of the least-squares fit to a straight line through the origin. This yields Al = 1.046 $\pm$ 0.006, χ^2 = 22.2 for 19 degrees of freedom, and $P(\chi^2) \simeq$ 0.27. The fit is satisfactory and suggests that MONTE predicts the relative variation of δ_{28} with cluster geometry and coolant density to within the $\sim \pm 2$ per cent accuracy with which the trend can be established by optimum use of the experimental results.

6. COMPARISON OF MONTE AND WIMS CALCULATIONS

Table 1 shows that WIMS calculations, with the options detailed in section 3.5, give very similar cluster average δ_{28} values to the MONTE calculation with the basic ^{238}U cross section data from the METHUSELAH December 1964 library.

The WIMS results show very similar trends with geometry and coolant changes to those given by MONTE, and on average are about one and a half per cent higher, that is, closer to the experimental results.

Since both METHUSELAH and the DSN option of WIMS use a ring-smearing technique for the cell neutron flux calculation, this is further evidence that the failure of METHUSELAH to predict satisfactorily the changes in δ_{28} with changing cluster geometry and coolant is attributable to the inadequacy of diffusion theory for calculating the fast flux variation across the cell, rather than to shortcomings of the ring-smearing approach.

7. CONCLUSIONS

1. A satisfactory method has been devised to correct MONTE calculations of δ_{28} for the effect of dissimilar surrounding lattice cells encountered in the experimental environment of the ZERLINA reactor. The required corrections are always acceptably small, being at most 0.6 per cent in δ_{28}.

2. The experimental results of Rose et al. have been re-analysed to provide more accurate definition of the experimental trend of cluster-average δ_{28} with cluster geometry and coolant density. The MONTE code has been shown to predict these trends to within the experimental relative accuracy of approximately $\pm$ 2 per cent.

3. The comparison of individual rod δ_{28} values between experiment and MONTE calculation shows no obvious trend with position in the cluster. Even if a trend were present, it would be difficult to observe owing to the rather low accuracy of the individual rod experimental results.

4. In the presently analysed series of experiments, there is no significant systematic difference in degree of agreement with MONTE between the 7-rod cluster data and that for larger clusters. This is in contrast with the previously published comparison (McCulloch, Doherty and Hesse, 1968) between MONTE and then existing experimental data, in which Canadian (Bigham, 1965)

data for 7-rod clusters showed a difference of some 8 per cent in measure of agreement with MONTE compared with the situation for larger clusters. This lends support to the possibility that an undetected systematic source of error may have been present in the Canadian experiments.

5. The relationship between the cluster-average data of Rose et al. and the MONTE calculated values is well described by

$$\delta_{28}(\text{expt}) = (1.05 \pm 0.01)\delta_{28}(\text{MONTE})$$

The slope of the line is rather less than that (1.08) found by McCulloch, Doherty and Hesse (1968). An overall assessment of the present and previous data is clearly indicated, and will form the basis of a separate report.

6. WIMS calculations using the DSN option for cell neutron transport, give cluster average δ_{28} values showing very similar trends with geometry and coolant changes to those given by MONTE. The WIMS values are on average about 1-1/2 per cent higher and 1-1/2 per cent closer to the experimental values than the MONTE values calculated using the basic METHUSELAH library ^{238}U cross section data. This is interpreted as further evidence that the failure of METHUSELAH to predict δ_{28} trends accurately lies in the failure of diffusion theory to calculate the variation of fast neutron flux in the lattice cell, rather than to an inherent deficiency of the ring-smearing model of the cluster.

8. ACKNOWLEDGEMENTS

The cooperation of Mr. A. Rose in detailed discussion of this experimental data, and his assistance in its re-analysis to suit the requirements of the present study is gratefully acknowledged. Mr. G. Robinson advised on many aspects of using the WIMS code, and Mr. L. Sullivan assisted with the regression line least-squares fitting.

9. REFERENCES

Alpiar, R. (1964) - UKAEA Report, AEEW-R135.

Askew, J.R., Fayers, F.J. and Kemshell, P.B. (1966) - J. Brit. Nuc. En. Soc. 5 (4), 564.

Bigham, C.B. (1965) - AECL Report, AECL 2285.

Brinkworth, M.J. and Griffiths, J.A. (1966) - UKAEA Report, AEEW-R480.

Hassitt, A. (1962) - UKAEA Report TRG-229(R).

McCulloch, D.B., Doherty, G. and Hesse, E.W. (1968) - J. Brit. Nuc. En. Soc. 7 (4), 307.

Pollard, J.P. and Robinson, G.S. (1966) - AAEC/E147.

Rose, A., Jain, H.M. and Menezes, P.F. (1972) - AAEC/E227.

Spinks, N. and Manning, G.E. (1967) - AAEC/E174.

Yiftah, S., Okrent, D. and Moldauer, P.A. (1960) - Fast Reactor Cross Sections - Pergamon Press, London and New York.

TABLE 1

Experimental and Calculated Cluster Average δ_{28} Values

Cluster			$10^4\ \delta_{28}$	$10^4\ \delta_{28}$ (calculated)				
No. of Rods	Spacing	Coolant	Exp.	METH/CRAM (pseudo-∞)	METH/CRAM (ZERLINA)	MONTE (reflected cell)	MONTE (corrected)	WIMS (corrected)
7	Standard	Air	310±12	216.9	216.8	311	311±4	316
		LD	324±12	216.8	216.8	306	306±4	313
		HD	303±12	216.0	216.0	302	302±4	312
		H_2O	308±13	209.2	209.3	300	300±4	303
7	Expanded	Air	263±11	155.1	154.6	246	245±4	254
		H_2O	231±12	133.3	133.7	221	222±3	218
19	Standard	Air	466±18	439.7	438.9	453	452±3	457
		LD	478±18	433.6	433.1	448	447±3	452
		HD	459±17	422.8	422.5	433	433±3	441
		H_2O	440±17	396.1	396.1	412	412±2	417
19	Expanded	Air	406±15	330.5	328.7	378	376±3	379
		LD	367±14	318.8	317.9	356	355±3	363
		HD	354±15	297.0	296.9	336	336±3	344
		H_2O	329±14	251.3	251.9	307	308±3	309
37	Standard	Air	638±21	651.3	649.1	589	587±3	594
		LD	611±24	631.0	629.4	572	571±3	577
		HD	586±21	598.2	597.4	548	547±3	552
		H_2O	514±23	536.2	536.2	499	499±2	509
61	Standard	Air	768±26	899.8	896.6	729	726±3	737
		H_2O	611±22	735.9	735.4	609	609±2	617

TABLE 2

Comparison of Experimental and MONTE δ_{28} Values for Each Cluster Ring

Cluster	Coolant	$10^4\ \delta_{28}$									
		Centre		Ring 1		Ring 2		Ring 3		Ring 4	
		Exp.	Calc.	Exp.	Calc.	Exp.	Calc.	Exp.	Calc.	Exp.	Calc.
7S	Air	364±11	388	302± 7	298						
	LD	389±12	392	316± 7	294						
	HD	399±12	395	289± 7	289						
	H_2O	400±13	419	291± 7	285						
7E	Air	304±10	273	259± 6	246						
	H_2O	304±11	293	225± 7	215						
19S	Air	611±19	607	573±18	558	409±13	404				
	LD	682±20	666	605±18	580	418±13	385				
	HD	709±20	700	590±17	586	399±12	366				
	H_2O	678±20	688	600±18	590	372±12	346				
19E	Air	495±15	474	475±14	443	370±12	348				
	LD	519±15	496	440±13	439	328±11	313				
	HD	542±16	491	482±15	448	304±11	287				
	H_2O	512±16	462	459±14	416	280±10	264				
37S	Air	939±26	933	888±25	873	769±21	700	500±11	457		
	LD	949±27	1019	892±27	891	762±24	709	468±11	438		
	HD	1043±29	993	943±28	903	741±22	706	443±10	411		
	H_2O	1007±30	994	949±28	876	694±20	674	380±10	366		
61S	Air	1286±35	1347	1246±35	1250	1112±31	1079	839±16	818	547±10	506
	H_2O	1405±39	1268	1321±39	1209	1010±30	1024	721±16	736	410± 8	407

TABLE 3

Group Energy Boundaries for Cell Transport Calculations in WIMS

Group	Lower Energy Boundary (eV)
	10^7
1	3.679×10^6
2	8.210×10^5
3	6.734×10^4
4	5.530×10^3
5	48.052
6	27.700
7	9.877
8	4.000
9	1.071
10	0.996
11	0.625
12	0.350
13	0.220
14	0.100
15	0.050
16	0.030
17	0.015
18	0

TABLE 4

Details of Least-Squares Fitting to Cluster Average δ_{28} Results of Rose et al.

X δ_{28} (MONTE)	Y δ_{28} (EXPT)	DY $\sigma[\delta_{28}$ EXPT]	Y_{FIT} δ_{28} (FIT)	$\frac{(Y-Y_{FIT})^2}{(DY)^2}$
3.110000E+02	3.100000E+02	1.300000E+01	3.264570E+02	1.602566E+00
3.060000E+02	3.240000E+02	1.300000E+01	3.212085E+02	4.610943E-02
3.020000E+02	3.030000E+02	1.300000E+01	3.170098E+02	1.161382E+00
3.000000E+02	3.080000E+02	1.400000E+01	3.149104E+02	2.436410E-01
2.450000E+02	2.630000E+02	1.200000E+01	2.571768E+02	2.354870E-01
2.220000E+02	2.310000E+02	1.200000E+01	2.330338E+02	2.872368E-02
4.520000E+02	4.660000E+02	1.800000E+01	4.744651E+02	2.211657E-01
4.470000E+02	4.780000E+02	1.800000E+01	4.692166E+02	2.381140E-01
4.330000E+02	4.590000E+02	1.700000E+01	4.545208E+02	6.942439E-02
4.120000E+02	4.400000E+02	1.700000E+01	4.324771E+02	1.958296E-01
3.760000E+02	4.060000E+02	1.500000E+01	3.946877E+02	5.687428E-01
3.550000E+02	3.670000E+02	1.400000E+01	3.726440E+02	1.625265E-01
3.360000E+02	3.540000E+02	1.500000E+01	3.526997E+02	7.514495E-03
3.080000E+02	3.290000E+02	1.400000E+01	3.233081E+02	1.652942E-01
5.870000E+02	6.380000E+02	2.100000E+01	6.161748E+02	1.080133E+00
5.710000E+02	6.110000E+02	2.400000E+01	5.993796E+02	2.344319E-01
5.470000E+02	5.860000E+02	2.100000E+01	5.741868E+02	3.164455E-01
4.990000E+02	5.140000E+02	2.300000E+01	5.238010E+02	1.815881E-01
7.260000E+02	7.680000E+02	2.600000E+01	7.620833E+02	5.178684E-02
6.090000E+02	6.110000E+02	2.200000E+01	6.392683E+02	1.651027E+00

δ_{28} (EXPT) = (1.050 ± 0.010) δ_{28}(MONTE)

$\sum \frac{(Y-Y_{FIT})^2}{(DY)^2}$ = 8.5 for 19 degrees of freedom

$P(\chi^2)$ ≃ 0.98

TABLE 5

Details of Least-Squares Fitting to Modified (Removal of Systematic Error Component) Cluster Average δ_{28} Results of Rose et al.

X1 δ_{28} (MONTE)	Y1 δ_{28} (EXPT)	DY1 $\sigma[\delta_{28}(\text{EXPT})]$	$Y1_{FIT}$ δ_{28} (FIT)	$\frac{(Y1-Y1_{FIT})^2}{(DY1)^2}$
3.110000E+02	3.090000E+02	8.700000E+00	3.254126E+02	3.558902E+00
3.060000E+02	3.250000E+02	9.000000E+00	3.201809E+02	2.867115E-01
3.020000E+02	3.030000E+02	8.400000E+00	3.159954E+02	2.393415E+00
3.000000E+02	3.060000E+02	8.400000E+00	3.139028E+02	8.851297E-01
2.450000E+02	2.640000E+02	7.599999E+00	2.563538E+02	1.012205E+00
2.220000E+02	2.290000E+02	6.500000E+00	2.322881E+02	2.558960E-01
4.520000E+02	4.670000E+02	1.310000E+01	4.729468E+02	2.060728E-01
4.470000E+02	4.770000E+02	1.350000E+01	4.677151E+02	4.730292E-01
4.330000E+02	4.600000E+02	1.280000E+01	4.530664E+02	2.934248E-01
4.120000E+02	4.390000E+02	1.240000E+01	4.310930E+02	4.066101E-01
3.760000E+02	4.080000E+02	1.160000E+01	3.934248E+02	1.578748E+00
3.550000E+02	3.690000E+02	1.060000E+01	3.714517E+02	5.349446E-02
3.360000E+02	3.550000E+02	1.030000E+01	3.515710E+02	1.108279E-01
3.080000E+02	3.270000E+02	9.700000E+00	3.222734E+02	2.374364E-01
5.870000E+02	6.410000E+02	1.380000E+01	6.142031E+02	3.770597E+00
5.710000E+02	6.080000E+02	1.350000E+01	5.974617E+02	6.093629E-01
5.470000E+02	5.840000E+02	1.330000E+01	5.723494E+02	7.763543E-01
4.990000E+02	5.130000E+02	1.220000E+01	5.221250E+02	5.594305E-01
7.260000E+02	7.610000E+02	1.350000E+01	7.596448E+02	1.007755E-02
6.090000E+02	6.110000E+02	1.210000E+01	6.372227E+02	4.696590E+00

$\delta_{28}(\text{EXPT}) = (1.046 \pm 0.006)\ \delta_{28}(\text{MONTE})$

$\sum \frac{(Y1-Y1_{FIT})^2}{(DY1)^2} = 22.2$ for 19 degrees of freedom

$P(\chi^2) \simeq 0.27$

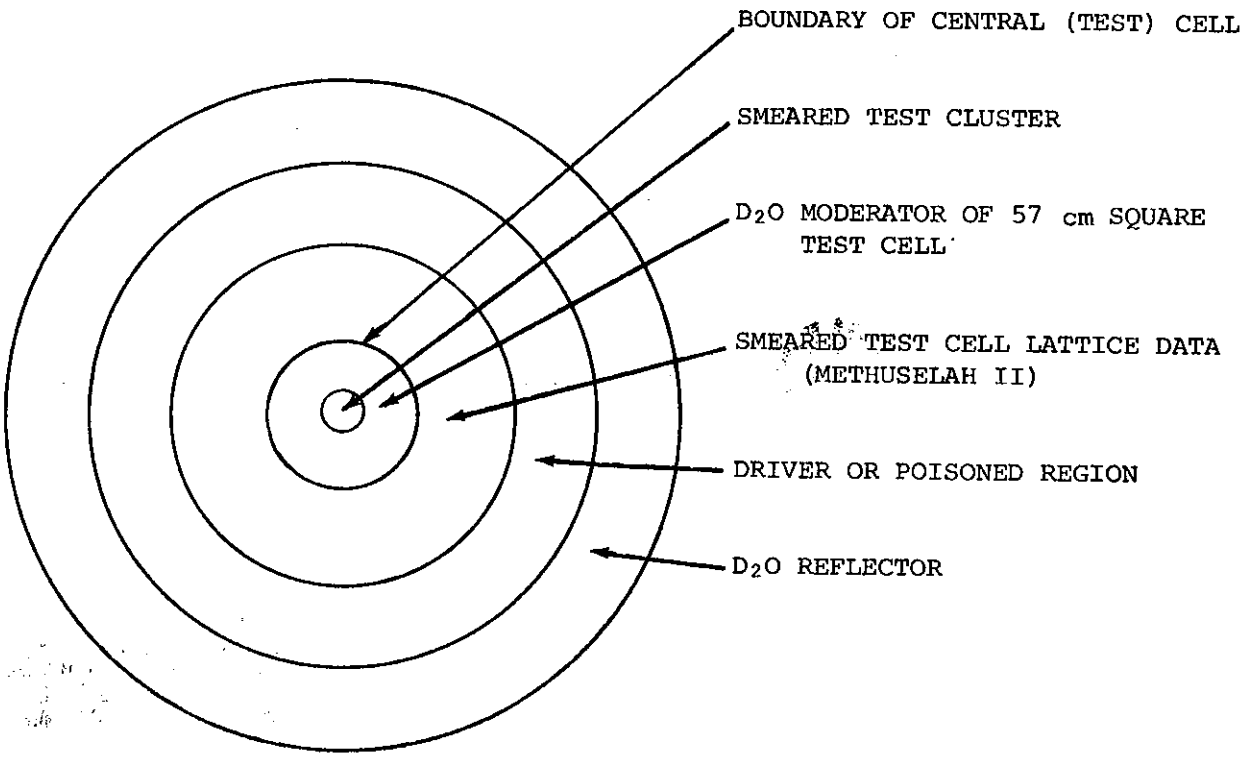

FIGURE 1a GENERAL ARRANGEMENT OF REGIONS USED IN VARIOUS CYLINDRICAL GEOMETRY CRAM ∞-LATTICE CALCULATIONS

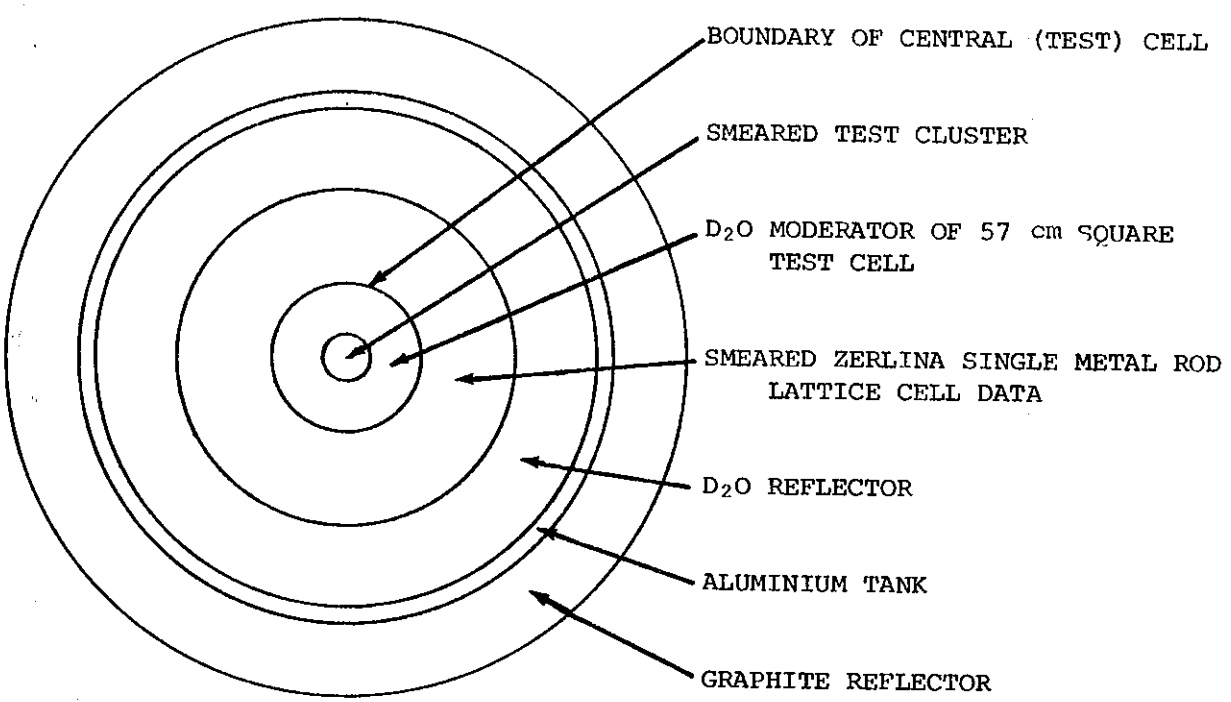

FIGURE 1b GENERAL ARRANGEMENT OF REGIONS USED IN CRAM CYLINDRICAL GEOMETRY REPRESENTATION OF ZERLINA

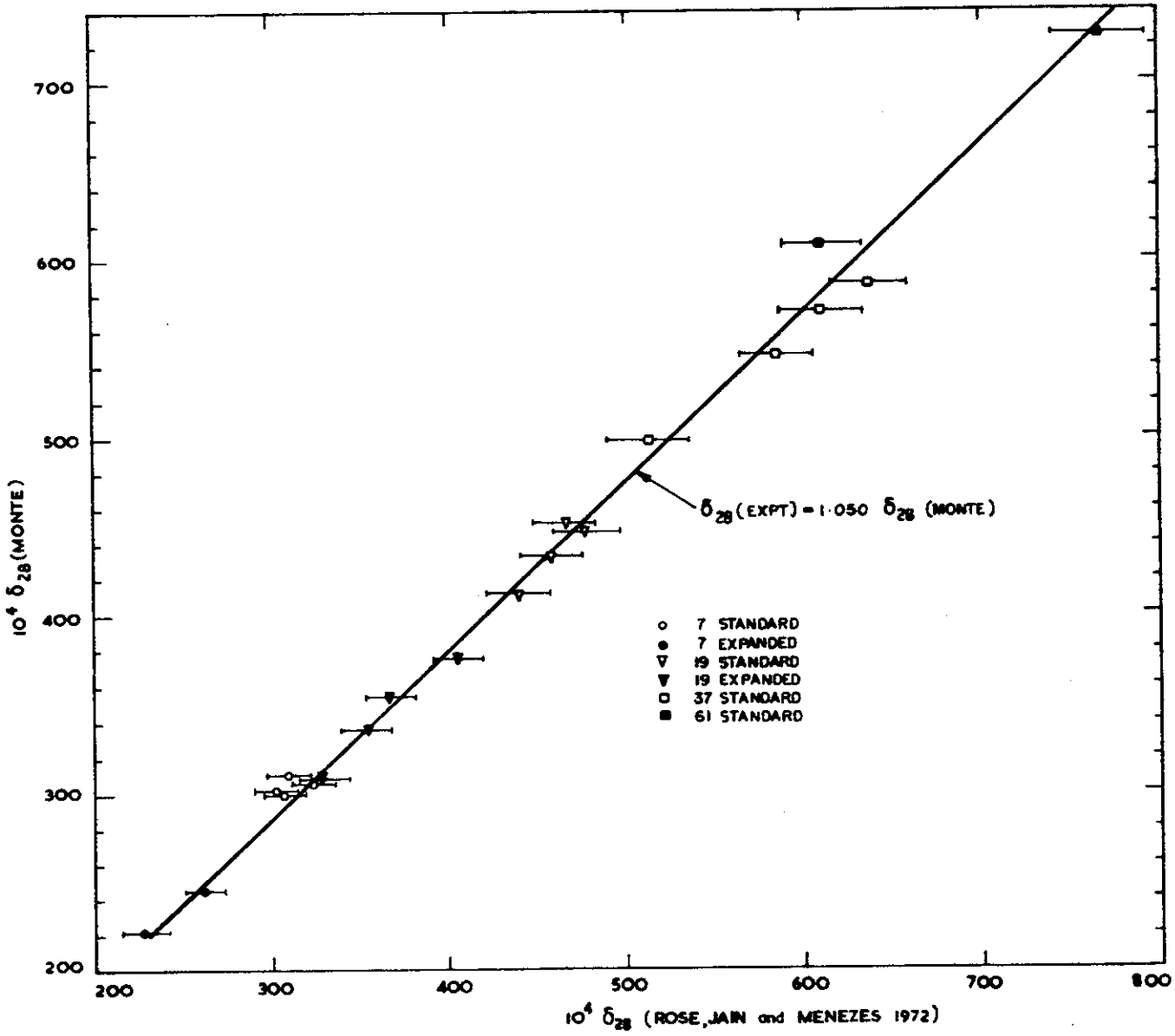

FIGURE 2. CLUSTER AVERAGED δ_{28} VALUES COMPARED WITH MONTE CALCULATIONS